PHYSICAL REVIEW A **76**, 011201(R) (2007)

Experimental observation and computational identification of $Sc@Cu_{16}^+$, a stable dopant-encapsulated copper cage

Nele Veldeman,[1] Tibor Höltzl,[2] Sven Neukermans,[1] Tamás Veszprémi,[3] Minh Tho Nguyen,[2] and Peter Lievens[1,*]

[1]*Laboratory of Solid State Physics and Magnetism and INPAC–Institute for Nanoscale Physics and Chemistry, K.U.Leuven, Celestijnenlaan 200D, B-3001 Leuven, Belgium*

[2]*Department of Chemistry and INPAC–Institute for Nanoscale Physics and Chemistry, K.U.Leuven, Celestijnenlaan 200F, B-3001 Leuven, Belgium*

[3]*Department of Inorganic and Analytical Chemistry, Budapest University of Technology and Economics, Szent Gellért tér 4, H-1111 Budapest, Hungary*

(Received 16 March 2007; published 5 July 2007)

We report a combined experimental and computational study of scandium doped copper clusters. The clusters are studied with time-of-flight mass spectrometry after laser fragmentation. Enhanced stabilities for specific cluster sizes in the mass abundance spectra are discussed using both electronic (shell closing) and geometric (symmetry) arguments. The exceptional stability observed for $Cu_{16}Sc^+$ is investigated in detail computationally. Density functional geometry optimizations at the Becke-Perdew 1986–LANL 2-double-zeta (BP86/LANL2DZ) level result in a Frank-Kasper tetrahedron, encapsulating a scandium atom in a highly coordinated position. The high stability is therefore interpreted in terms of extremely stable dopant encapsulated structures featuring a closed electron shell. The thermodynamic stability, as indicated by the stable backbone and large binding energy per atom, the relatively small ionization energy, and the moderate electron affinity of the neutral $Cu_{16}Sc$ cluster show that it has a superatom character, chemically similar to the alkaline-metal atoms.

DOI: 10.1103/PhysRevA.76.011201 PACS number(s): 36.40.Mr, 36.40.Qv, 61.46.Bc

Copper, silver, and gold clusters have been extensively studied over the last two decades. Among them, gold clusters attracted most attention, not in the least because of their unexpected geometric structures that have been identified in recent years. While small gold clusters were found to form planar structures up to fairly large sizes (Au_N^-, $N \leqslant 12$) [1,2], symmetric cage structures have been computationally predicted for larger species [3–6]. Because of the analogy with carbon clusters, which can form structures as diverse as chains, rings, graphene sheets, cages (fullerenes), and tubes (nanotubes), the term "golden fullerenes" quickly arose. More recently experimental evidence for the existence of hollow Au_N ($N=16-18,20$) cages was deduced from potential energy surface (PES) data [7]. Calculations suggest that these cages can easily accommodate a guest atom with very little structural distortion; $M@Au_N$ ($N=9-17$) obeying the 18 electron rule, were predicted computationally [8,9]. Starting from $N=9$, the heteroatom (M) prefers to be entirely surrounded by gold atoms to attain the lowest energy structure. In particular, WAu_{12}, $ZrAu_{14}$, $ScAu_{15}$, and YAu_{15} stand out in stability, as concluded by their high binding energy per atom (>2.40 eV) and large highest-occupied-molecular-orbital- (HOMO) lowest-unoccupied-molecular-orbital (LUMO) gap (>1.70 eV). The latter explains the very large abundances observed experimentally for the isoelectronic cations YAu_{16}^+ and $ScAu_{16}^+$, in previously reported photofragmentation studies [10,11].

Concerning silver clusters, a combined experimental and computational study attributes the enhanced stability observed for $Ag_{10}Co^+$ to a symmetric structure of ten silver atoms surrounding the central Co atom, whose magnetic moment is completely quenched [12]. Among the slightly larger sizes, exceptional stabilities were recorded for $Ag_{14}V^+$, $Ag_{15}Ti^+$, and $Ag_{16}Sc^+$.

As its higher mass congeners silver and gold, copper clusters have been studied extensively starting from the early years of metal cluster physics until today [13–18]. Simultaneously, transition metal doped copper clusters are intensively considered computationally [19–24], mainly because of the interest in the local magnetism in dilute systems of magnetic impurities in nonmagnetic metals (Kondo effect). Experimental information, however, is very scarce [25,26].

In this paper we report the size dependent stability of scandium doped copper clusters Cu_NSc^+, which are produced in a dual-target dual-laser vaporization source. Stability patterns follow from photofragmentation mass spectrometry and are discussed in terms of the phenomenological shell model. The exceptional stability observed for $Cu_{16}Sc^+$ is studied computationally in detail using density functional theory at the BP86/LANL2DZ level.

For the production of (doped) copper clusters, the dual-target dual-laser vaporization source [27] was operated at liquid nitrogen temperature. The source parameters (gas pressure, laser powers, time delays between the opening of the gas valve and the firing of the lasers) are carefully optimized for stable production of copper clusters containing only a few dopant atoms. After passing a skimmer, the cluster beam is irradiated with high fluence laser light stemming from an ArF excimer laser ($\lambda=193$ nm, >5 mJ_{pp}/cm^2). The clusters are heated by multiphoton absorption and cooling occurs through the sequential evaporation of atoms, ions, or even larger fragments in the extraction region. Following the acceleration in the extraction zone, the fragments are mass

*Electronic address: peter.lievens@fys.kuleuven.be

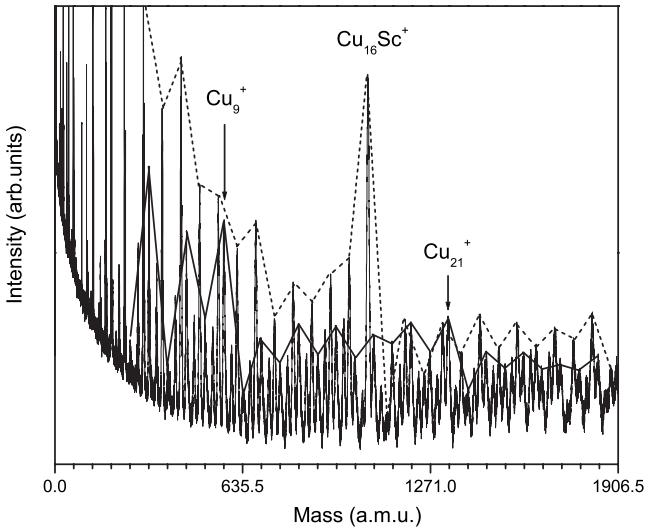

FIG. 1. Mass abundance spectrum of scandium doped copper clusters (Cu_NSc^+, $N=1-30$) recorded with the cluster source operating at liquid nitrogen temperature and following high fluence irradiation with an ArF excimer ($\lambda=193$ nm, >5 mJ_{pp}/cm^2). The mass peaks connected with a solid line correspond to pure Cu_N^+ clusters. Singly doped species are connected by a dashed line.

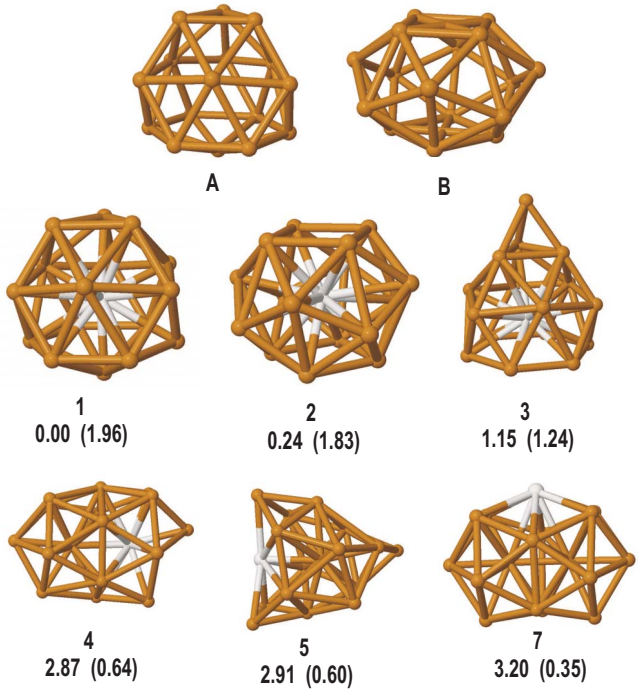

FIG. 2. (Color online) The geometrical structures of the most stable clusters and their relative energies (in eV, compared to the most stable structure), and the vertical singlet-triplet gaps (in eV, indicated in parentheses). The scandium atom is indicated by light gray spheres.

separated in the field free drift region of the reflectron time-of-flight mass spectrometer and detected by a dual microchannel plate detector. The resulting photofragmentation spectra reveal a size distribution with higher abundances for clusters with an enhanced stability (see Ref. [28], and references therein).

The photofragmentation mass spectrum for Cu_NSc^+ ($N=1-30$) is shown in Fig. 1. Pure Cu_N^+ clusters are connected with a solid line and steps in abundance after $N=9$, 21, 41, and 59 (41 and 59 not in the figure) are observed, in agreement with earlier investigations and corresponding to the known electronic shell structure with shell closings at a total number of 8, 20, 40, and 58 delocalized valence $4s$ electrons [13]. Next to peaks stemming from pure copper clusters also peaks corresponding to singly and doubly scandium doped clusters are visible. In this work, we focus on the singly doped Cu_NSc^+ clusters (dashed line in Fig. 1). The abundance spectrum reveals pronounced peaks and steps after specific cluster sizes. Enhanced abundances are observed for Cu_6Sc^+ and $Cu_{16}Sc^+$. Assuming that each copper atom, as for pure Cu_N^+ clusters, delocalizes its $4s$ electron, these sizes correspond to the magic numbers 8 and 18 for electronic shell closing ($1s^2/1p^6/1d^{10}$) provided that the Sc atom delocalizes its three valence electrons ($3d^14s^2$). While the magic number 8 is also observed for pure Cu_N^+ clusters, 18 is not. Instead the magic number 20 occurs for pure Cu_N^+. The shift from 20 to 18 valence electrons induced by Sc doping can be interpreted in a two-step phenomenological shell model for doped metal clusters [29]. The corresponding enhanced energy gap between the $1d^{10}$ and $2s^2$ spherical levels originates from a central increase in the background potential stemming from a more electropositive central dopant compared to its surrounding host atoms. A central hump in the background potential is disadvantageous for orbitals with central electron density (s levels). As such, the 20 to 18 magic number shift suggests that the Sc dopant (which is less electronegative than Cu) holds a central position in the $Cu_{16}Sc^+$ cluster.

Because of its exceptional stability, the $Cu_{16}Sc^+$ cluster is investigated computationally in more detail. Computations were performed by the GAUSSIAN03 quantum chemical program package [30]. Geometries were optimized without constrains, and harmonic vibrational frequencies were computed using the Becke-Perdew 1986–LANL 2-double-zeta BP86/LANL2DZ level of theory [31–33] which has been chosen by comparison with *ab initio* computations on a Cu_3Sc cluster (see the supplementary material for details [34]). Our test computations on Cu_2 show excellent agreement with the experimental results [35]: bond length $d_{calc}=2.230$ Å ($d_{expt}=2.220$ Å), vibrational frequency $\omega_{calc}=274.6$ cm^{-1} ($\omega_{expt}=264.5$ cm^{-1}), and binding (cohesive) energy $D_{e,calc}=2.04$ eV ($D_{e,expt}=1.97$ eV). The density of states (DOS) was computed by the PYMOLYZE code [36], while the C-squared [37] population analysis was used for fragment DOS computation. Natural bond orbital (NBO) analysis was performed by the NBO3.0 [38] code built into the GAUSSIAN program. Due to the large number of atoms in this cluster, it is not possible to locate all the minima on the PES. However, we have carried out an extensive study to find the stable clusters, as described in the supplementary material. The most stable minima together with the relative energies (compared to the lowest energy cluster) and the vertical singlet-triplet gaps are available in Fig. 2. Other structures are available in the supplementary material [Fig. 2(S)]. The most stable geometric structure, i.e., the lowest energy structure, is

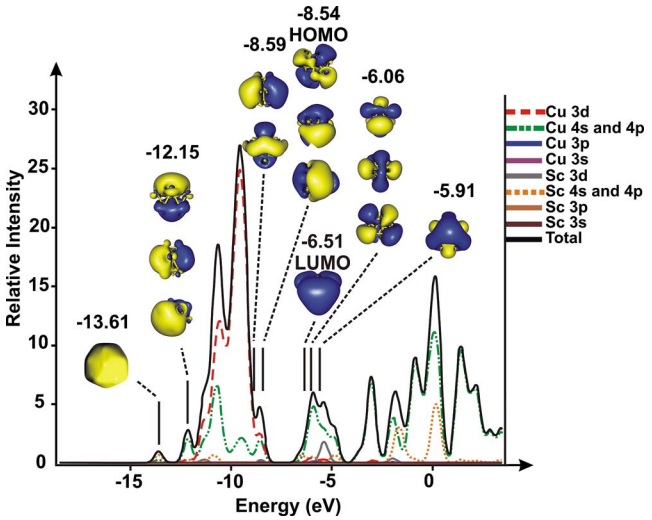

FIG. 3. (Color online) The total and fragment density of states of the T_d symmetric $Cu_{16}Sc^+$ cluster 1. The Kohn-Sham molecular orbital energies are indicated in eV.

labeled with 1, while structure 14 has the highest energy. All the compounds have only real vibrational frequencies, and due to the positive vertical singlet-triplet gap, it is expected that the triplet PES lies above the singlet. According to our computations, the most stable cluster is the T_d symmetry Frank-Kasper tetrahedron (cluster 1), which also has been reported by *ab initio* computations on $Au_{16}Si$ [39]. However the second (cluster 2) is lying higher by only 0.24 eV (0.19 eV at the more accurate BP86/Stuttgart RSC 1997 level of theory [40]), and therefore it is expected that during the experiments, both clusters can be formed. To ensure that their ground state is singlet, we computed the adiabatic singlet-triplet gaps, which are 1.88 and 1.67 eV for clusters 1 and 2, respectively.

The most stable clusters have endohedral scandium. The relative energies of the clusters increase if the scandium atom is placed outside the copper-cage (as in the 5, 6, 7, 8, and 14 clusters), while the relative energy is much lower if the scandium remains endohedral and only the copper atoms are rearranged (as in cluster 3). This suggests that scandium prefers a large coordination number. Consistently, the total Wiberg bond index (i.e., the valency) of scandium atom is 6.5 in the case of cluster 1, while it is 1.3–1.4 (depending on the position) in the case of copper atoms. This can be explained by the electron donation from the copper to the *d* orbitals of scandium: according to the NBO analysis, the natural electronic configuration of the valence shell of copper atoms slightly changes depending on the position and is approximately $[Ar]4s^{0.8}3d^{9.9}5p^{0.05}$, while it is $[Ar]4s^{0.8}3d^{5.9}4d^{0.1}5p^{0.3}$ for the scandium. Consistently, cluster 4 with an endohedral scandium atom is more stable than its analogs where the scandium is on the surface of the cluster (7, 9, 10, 11, 12, 13).

Now we will focus on the electronic structure and properties of the most stable (T_d symmetry, structure 1) $Cu_{16}Sc^+$ cluster. Figure 3 shows the total and fragment DOS of $Cu_{16}Sc^+$, and some important assigned molecular orbitals. The fragment DOS shows that the low-energy part of the band (up to −12 eV) is formed mainly by the 4*s* orbitals of copper and scandium. The next two large peaks (at −10.9 and −9.8 eV)—consistent with the NBO analysis—mainly consist of the 3*d* orbitals, however, the contribution from the 4*s* electrons is also noteworthy. The remaining occupied orbitals have considerably high contributions from both the 4*s* and 4*p*, and the 3*d* orbitals of the copper cage. We have assigned the orbitals which posses most shell model character, i.e., the orbitals that correspond to peaks with considerably high 4*s* contribution. These orbitals involve 18 electrons in total, in agreement with the experimental stability of $Cu_{16}Sc^+$. The shape of the orbitals corresponding to the two large peaks also resembles that from the shell model and they are also localized at the surface of the cluster; however, due to the large contribution of the *d*-atomic orbitals, they are not as diffuse as the orbitals shown on Fig. 3. The t_2 HOMO and the *e* symmetry HOMO-1 are quasidegenerate (E=0.05 eV), showing clearly that these five orbitals correspond to the 1*d* shell of the cluster. The relatively large HOMO-LUMO gap (2.05 eV) shows the stability of this cluster and is consistent with the 1.96 eV vertical singlet-triplet separation.

According to the shell model, the Cu_{16}^{2-} structure is isoelectronic with the $Cu_{16}Sc^+$ cluster, both have a closed $1s^2/1p^6/1d^{10}$ electronic configuration. Moreover, similar to cluster 1, its hollow Cu_{16}^{2-} analog (labeled by A in Fig. 2) is a minimum on the PES. The similarity of their electronic structure is also reflected by the occupied part of the density of states (shown in Fig. 3S in the supplementary material). The HOMO-LUMO gap (0.98 eV) is a factor of 2 smaller than in the case of $Cu_{16}Sc^+$, which implies that the scandium dopant atom increases the stability of the cluster.

According to the Nucleus Independent Chemical Shift (NICS) in the center of the Cu_{16}^{2-} cage (−65.5 ppm) and the closed electronic shell structure, similar to the previously reported I_h symmetrical fullerenes, structure A can be spherically aromatic [41], which induces the stability of the isoelectronic cluster 1. Similarly, the backbone of $Au_{16}Si$ is the Frank-Kasper tetrahedron-shaped Au_{16}^{2-} dianion [39]. The hollow Cu_{16}^{2-} analog of structure 2 (B in Fig. 2), however, is a second-order saddle point on the PES, the NICS in the center of the cage is −60.8 ppm, inducing also a spherically aromatic character. According to Ref. [42], the endohedral dopant atom stabilizes the cluster, therefore the doped derivative becomes a minimum on the PES.

The neutral $Cu_{16}Sc$ cluster involves 19 electrons on the orbitals corresponding to the shell model. According to this, the electronic structure can be stabilized by electron detachment (reaching the 18 electron closed shell configuration) or electron attachment (leading to the stable 20 electron configuration). According to the very small adiabatic ionization energy [5.03 eV, comparable to the 5.14 eV value of lithium and even smaller than the 5.8 (5.9) eV value for the Cu_{16} (Cu_{17}) cluster [43]] and the relatively large electron affinity (1.95 eV on the (BP86/LANL2DZ) level of theory, and 2.07 eV using the BP86/6-311++G^{**} method, larger than the 0.62 eV of the lithium atom, and similar to the 1.43 eV first electron affinity of oxygen), both can be feasible processes. The binding energy per atom (−2.62 eV) is also larger than the −2.2 (−2.3) eV value for Cu_{16} (Cu_{17}) indicat-

ing the thermodynamic stability of this cluster. Therefore it is expected that this cluster has a superatom behavior, chemically similar to the alkaline-metal atoms. Similar to the hollow Au_{16}^{2-}, Cu_{16}^{2-} is a robust backbone, which properties can be tuned by the dopant atom [39].

In conclusion, we reported the experimental discovery of exceptionally stable $Cu_{16}Sc^{+}$ clusters. Geometry optimizations at the BP86/LANL2DZ level of theory reveal that $Cu_{16}Sc^{+}$ is a Frank-Kasper tetrahedron, encapsulating the scandium atom in a highly coordinated position. Density of states computations confirmed the high stability by as well the relatively large (2.05 eV) HOMO-LUMO gap, as by the fact that the most diffuse orbitals involve 18 electrons in total. The relatively small ionization energy and moderate electron affinity calculated for the neutral $Cu_{16}Sc$ cluster suggest that it mimics the chemistry of the alkaline-metal atoms.

This work is supported by the Fund for Scientific Research-Flanders (FWO), the Flemish Concerted Action (Grant No. GOA/2004/02), and the Belgian Interuniversity Poles of Attraction (Grant No. IAP/P5/01) programs.

[1] F. Furche *et al.*, J. Chem. Phys. **117**, 6982 (2002).
[2] H. Häkkinen *et al.*, J. Phys. Chem. A **107**, 6168 (2003).
[3] W. Fa and J. Dong, J. Chem. Phys. **124**, 114310 (2006).
[4] M. P. Johansson, D. Sundholm, and J. Vaara, Angew. Chem., Int. Ed. **43**, 2678 (2004).
[5] Y. Gao and X. C. Zeng, J. Am. Chem. Soc. **127**, 3698 (2005).
[6] J. Wang *et al.*, J. Phys. Chem. A **109**, 9265 (2005).
[7] S. Bulusu *et al.*, Proc. Natl. Acad. Sci. U.S.A. **103**, 8326 (2006).
[8] Y. Gao, S. Bulusu, and X. C. Zeng, J. Am. Chem. Soc. **127**, 156801 (2005).
[9] Y. Gao, S. Bulusu, and X. C. Zeng, ChemPhysChem **7**, 2275 (2006).
[10] W. Bouwen *et al.*, Chem. Phys. Lett. **314**, 227 (1999).
[11] S. Neukermans *et al.*, Phys. Rev. Lett. **90**, 033401 (2003).
[12] E. Janssens *et al.*, Phys. Rev. Lett. **94**, 113401 (2005).
[13] I. Katakuse *et al.*, Int. J. Mass Spectrom. Ion Process. **67**, 229 (1985).
[14] O. Cheshnovsky *et al.*, Phys. Rev. Lett. **64**, 1785 (1990).
[15] M. B. Knickelbein, Chem. Phys. Lett. **192**, 129 (1992).
[16] M. L. Yang *et al.*, J. Chem. Phys. **124**, 024308 (2006).
[17] V. G. Grigoryan, D. Alamanova, and M. Springborg, Phys. Rev. B **73**, 115415 (2006).
[18] S. Li, M. M. G. Alemany, and J. R. Chelikowsky, J. Chem. Phys. **125**, 034311 (2006).
[19] P. Blaha and J. Callaway, Phys. Rev. B **33**, 1706 (1986).
[20] D. Bagayoko, P. Blaha, and J. Callaway, Phys. Rev. B **34**, 3572 (1986).
[21] Q. Sun *et al.*, Phys. Rev. B **54**, 10896 (1996).
[22] Q. Sun *et al.*, Phys. Lett. A **209**, 249 (1995).
[23] J. L. Ricardo-Chávez and G. M. Pastor, J. Magn. Magn. Mater. **294**, 122 (2005).
[24] E. Florez, F. Mondrágon, and P. Fuentealba, J. Phys. Chem. B **110**, 13793 (2006).
[25] P. Joyes and M. Leleyter, J. Phys. B **16**, 671 (1983).
[26] J. Van de Walle, P. Joyes, and P. Sudraud, J. Phys. C **12**, 211 (1984).
[27] W. Bouwen *et al.*, Rev. Sci. Instrum. **71**, 54 (2000).
[28] K. Hansen *et al.*, Phys. Rev. A **73**, 063202 (2006).
[29] E. Janssens, S. Neukermans, and P. Lievens, Curr. Opin. Solid State Mater. Sci. **8**, 185 (2004).
[30] GAUSSIAN 03, Revision C.01, M. J. Frisch *et al.* (Gaussian, Inc., Wallingford CT, 2004).
[31] A. D. Becke, Phys. Rev. A **38**, 3098 (1988).
[32] J. P. Perdew, Phys. Rev. B **33**, 8822 (1986).
[33] P. J. Hay and W. R. Wadt, J. Chem. Phys. **82**, 270 (1985).
[34] See EPAPS E-PLRAAN-75-R02706 for a detailed description of the methods of computations, and of geometry optimizations in particular. Next to the structures shown in Fig. 2, other computed isomers are listed. Moreover, the total and fragment DOS of $Cu_{16}Sc^{2-}$ and $Cu_{16}Sc$ are compared with the DOS of $Cu_{16}Sc^{+}$, shown in Fig. 3. For more information on EPAPS see http://www.aip.org/pubservs/epaps.html.
[35] A. Pasquarello *et al.*, Phys. Rev. Lett. **69**, 1982 (1992).
[36] Adam L. Tenderholt, PYMOLYZE: A Program to Analyze Quantum Chemistry Calculations, http://pymolyze.sourceforge.net
[37] CCLIB for parsing and interpreting the results of computational chemistry packages, http://cclib.sourceforge.net
[38] E. D. Glendening, A. E. Reed, J. E. Carpenter, and F. Weinhold, NBO Version 3.1 (unpublished).
[39] M. Walter and H. Häkkinen, Phys. Chem. Chem. Phys. **8**, 5407 (2006).
[40] Basis sets were obtained from the Extensible Computational Chemistry Environment Basis Set Database, Version 02/02/06. M. Dolg, U. Wedig, H. Stoll, and H. Preuss, J. Chem. Phys. **86**, 866 (1987), basis sets and ECPs correspond to Revision: Fri Jun 27 1997 of the Stuttgart/Dresden groups.
[41] A. Hirsch, Z. Chen, and H. Jiao, Angew. Chem., Int. Ed. **39**, 3915 (2000).
[42] Z. Chen *et al.*, J. Am. Chem. Soc. **128**, 12829 (2006).
[43] M. Yang *et al.*, J. Chem. Phys. **124**, 024308 (2006).